



ELSEVIER

Aquacultural Engineering 21 (1999) 33–48

aquacultural
engineering

www.elsevier.nl/locate/aqua-online

An optical method for the detection of sea lice, *Lepeophtheirus salmonis*

R.D. Tillett, C.R. Bull, J.A. Lines *

Silsoe Research Institute, Silsoe, Bedford, MK45 4HS, UK

Received 19 April 1999; accepted 29 June 1999

Abstract

Developments towards a novel video camera based system for estimating the sea lice burden of freely swimming salmon are reported. The spectral reflectance of sea lice and salmon skin were measured over the wavelength range 400–1100 nm. Canonical variate analysis was then used to identify a combination of reflectances that maximises the differences between skin and sea lice. This is shown to provide good discrimination when the lice are attached to the lighter underside of the fish and a degree of discrimination when the lice are attached to the darker areas. The results of this analysis were used to develop a simple video based discrimination system. An image of the salmon is synthesised from the ratio of grey levels of images taken through narrow band pass filters at wavelengths of 700 and 800 nm. This enhances the visibility of the lice and suppresses variations in the skin colour. Further development of this technique could lead to an automated passive system for estimating lice burden. © 1999 Elsevier Science B.V. All rights reserved.

1. Introduction

Sea lice are one of the most serious and costly diseases faced by the salmon industry. Estimates of the costs incurred due to lice vary widely but are likely to exceed £20 million per annum in both Scotland and Norway (Kvenseth, 1997; Sinnott, 1998; Smith, 1999). These costs are incurred through low growth and food conversion ratio, stock losses, secondary diseases and harvest price mark down as well as the costs of monitoring and treating the fish.

* Corresponding author. Tel.: +44-1525-860156; fax: +44-1525-860000.

E-mail address: jeff.lines@bbsrc.ac.uk (J.A. Lines)

The most wide spread sea louse is *Lepeophtheirus salmonis*. It has a life cycle which begins with several free swimming planktonic stages during which the lice are typically less than 1 mm long (Johnson and Albright, 1991). This is followed by chalimus stages where the lice are firmly attached to the salmon. At the end of these stages the lice are up to 2.5 mm long. The final stages comprise two pre adult stages and an adult stage. An adult louse is around 5–8 mm long with the female trailing egg sacks a further 6 or 8 mm in length. At a temperature of 10°C, development from an egg to a mature adult takes around 40 days for a male and 52 days for a female (Schram, 1993).

Infestation of salmon tends to begin with lice attaching themselves behind the dorsal fin. As infestation becomes heavier, the rest of the back, particularly the top of the head becomes colonised. Heavily infected fish also have lice on the lighter underside, tail and fins. The pre-adult and adult stages cause substantially more damage to the host than the earlier stages. Grimnes and Jakobsen (1996) suggest that infection intensities above 30 salmon lice larvae per fish may cause the death of Atlantic salmon post-smolt soon after the lice reach their pre-adult stage.

There exist a range of possible treatments for sea lice, none of which are entirely satisfactory. Most of these treatments rely on regular monitoring of lice numbers to identify the optimum time for treatment. In order to minimise the costs of this process, a rather small sample of fish are used and these are caught from the surface of the sea cage with minimal disruption to the salmon. (Bakke Jøssund, 1995; Jackson, 1998; Treasurer and Grant, 1998). It is to be expected that this sampling procedure gives rise to large uncertainty in the estimates of the lice burden.

The research reported in this paper indicates a method for enhancing the contrast between lice and fish skin by synthesising a video image from images captured at two specific wavelengths. This might allow automatic or manual estimation of the sea lice burden of freely swimming fish.

The reflection properties of fish skin and sea lice were first examined to identify spectral differences which might facilitate discrimination. The variation in reflectance from a material over a wavelength range due to the presence of different absorbing compounds can give an identifying signature that allows it to be distinguished from another material of similar colouration. This is a technique that has found a number of applications in the sorting and identifying of agricultural and food materials (Mohesenin, 1984; Bull, 1993; Bull et al., 1995). We show how observed differences in spectral reflection properties have been used to identify characteristic wavelengths which can be used to discriminate between lice and salmon skin.

Following this spectral analysis, video images were recorded at the characteristic wavelengths identified. These were then combined to synthesise an image in which discrimination between salmon skin and sea lice is substantially greater than in a normal video image.

This work has demonstrated the possibility of an underwater video based lice detection system. Further work is required to examine the variability the spectra over a larger sample of salmon and lice, to test the system on live salmon and to optimise and enhance the discrimination. If successful the resulting underwater

video based sensing system could replace manual sampling of the fish. This would lead to reductions in cost, labour and fish stress. Further, because it is a process that might be achieved with some level of automation and at a range of depths, it may provide a more accurate view of changes in the sea lice burden throughout the whole cage population.

2. Collection of spectral scans

Two sets of spectral scans were taken in this investigation. One set was used to characterise the light reflection and transmission properties of lice detached from the surface of the Atlantic salmon. A second set of scans was used to characterise the reflection properties of the lice on the surface of the salmon.

The reflectance measurements were made using the system illustrated in Fig. 1. This comprises a stabilised 100 W tungsten halogen light source, a bifurcated light guide and a monochromator. Light from the source was guided along one arm of the light guide onto the fish or lice and the reflected light was collected into the second branch of the light guide and taken into an optical spectrum analyser (Monolight Instruments 6101 device). In the bifurcated light guide (Monolight Instruments 3134) the fibres of the incoming and outgoing arms at the probe end are randomly mixed. Transmission measurements were made with the equipment configured as shown in Fig. 2. A fibre optic bundle conveyed light from the light source onto the sample. Transmitted light was collected and transferred to the spectrum analyser by a second set of fibres.

An optical spectrum analyser was used to examine the transmission and reflectance scans. The optical spectrum analyser splits the light into its component wavelengths using a diffraction grating and narrow entry and exit slits. In this case the slit widths were set up to give a spectral resolution of 2.5 nm. The scans were taken over a wavelength range of 380–1100 nm at 2-nm intervals. In order to minimise spectral noise, the response was determined by integrating the signal over 100 individual scans. In terms of light colour, 380 nm represents light at the violet

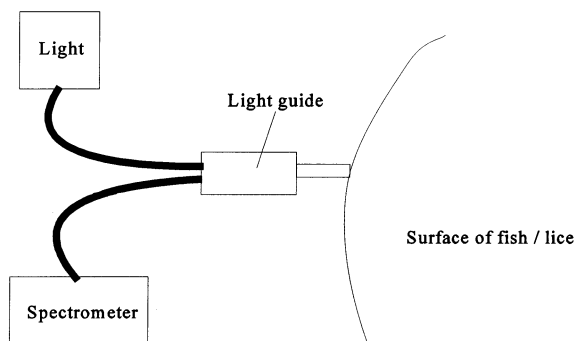


Fig. 1. Schematic diagram of the reflection measurement system.

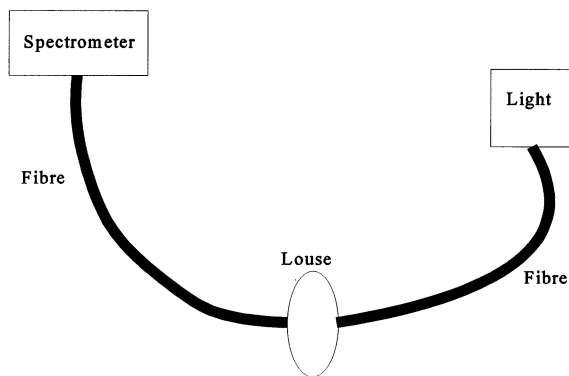


Fig. 2. Schematic diagram of the transmission measurement system.

end of the visible spectrum, while 1100 nm is near infrared light. The upper wavelength limit of the visible spectrum (red) occurs at a wavelength of about 780 nm (Hecht and Zajac, 1979)

The raw data from the optical spectrum analyser shows the optical response of the whole system and is therefore a function of the optical properties of the light source, guiding fibres, monochromator and detector as well as the optical properties of the sample. In order to determine the absolute reflectance or transmission characteristics of the sample alone, it is necessary to divide the measured spectrum by a reference spectrum obtained from either a fully reflective reference surface (for the reflectance measurements) or from the light that passes through the system with no sample present (for the transmission measurements). The reflective reference surface used in this work was Barium Sulphate, which is fully reflective in the visible and near infrared wavelengths.

Measurements of the reflection spectra of the detached lice were made on lice removed from a salmon which had been killed during a normal commercial harvest and held on ice for 24–36 h. Spectra were obtained under two conditions. In the first instance the lice were placed on the fully reflective reference surface. The bifurcated light probe illustrated in Fig. 1 was then placed in contact with each louse and the body reflectance determined. This was repeated for several lice. These measurements were then repeated with the lice placed on carbon black paper, in order to determine the level of reflectance from the lice when the material behind is strongly absorbing. Carbon black paper is extremely (and uniformly) absorbent in this wavelength range. Finally the transmission spectra of several different lice were determined by sandwiching each louse between narrowly separated fibre bundles as illustrated in Fig. 2.

Measurements of the reflection spectra of lice on the surface of the salmon were made on 30 lice from four salmon. These were made within 1 h of the fish being killed. The fish had not been cooled with ice. Measurements were taken by holding the bifurcated light probe in contact with these surfaces. Spectral reflectance measurements were also made of the fish skin adjacent to each of the lice. The

position of each louse on the fish was recorded. The lice on the fish and detached from the fish, were all in the adult or pre-adult stages. Most were female and several had trailing egg strings.

3. Description of spectral scans

3.1. Scans of detached sea lice

Typical reflectance scans for a detached sea louse are illustrated in Fig. 3. The upper curve shows the louse reflectance when it is placed upon a fully reflecting standard surface and the lower curve, when it is placed on absorbing carbon black

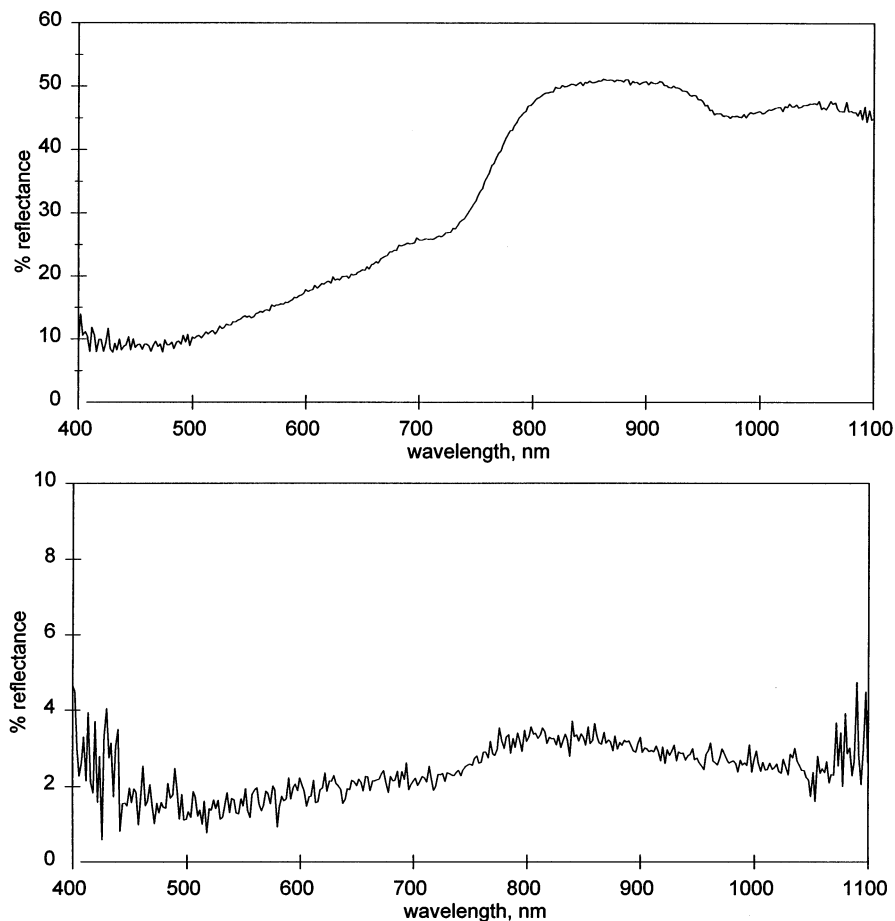


Fig. 3. Reflectance scan of a louse placed on a standard reflectance surface (upper) and on carbon black paper (lower).

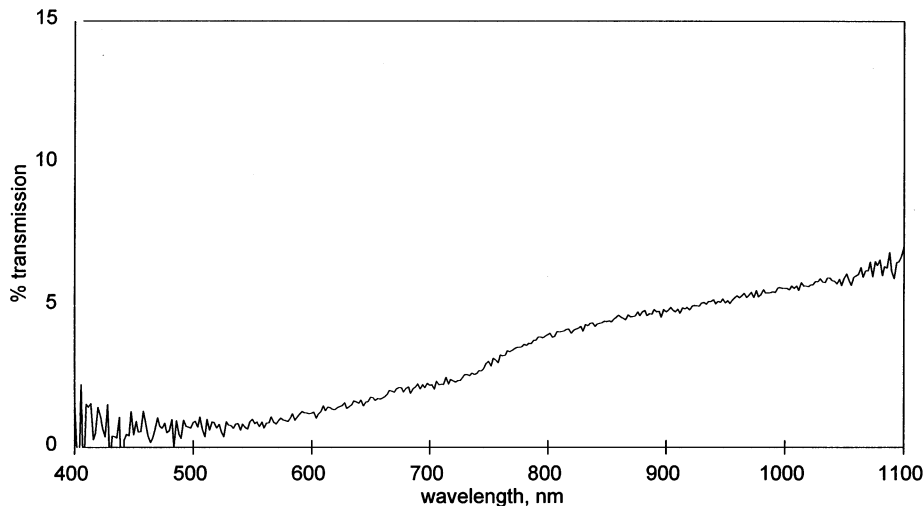


Fig. 4. Straight through transmission scan of a louse.

paper. The louse on the reflecting surface has a fairly steady increase in body reflectance from 400 to 850 nm reaching a maximum of around 50%. The reflectance then flattens out and starts to fall towards 1000 nm. The dip at around 1000 nm is probably due to water in the louse. Water has a strong and characteristic absorption band at 970 nm. The reflection scan for the same sea louse on the absorbing surface shows some of the same features with the reflectance increasing to a maximum at 850 nm, but the overall reflectance is much smaller and the absorption band at 970 nm is much less pronounced.

The difference in reflectance magnitude between the upper and lower graphs in Fig. 3 suggests that the absorption of lice is small, enabling the light to propagate through it into the surface behind. When there is a reflective surface behind the louse, the light is multiply scattered from the louse onto the reference surface and back so a substantial proportion of the light returns to the probe. The multiple passes of the light through the louse caused by scattering and reflection from the inner surface of the louse increases the average path length of the light in the louse and so emphasises any absorption features (Bull, 1990, 1991). This is evident in the more pronounced dip due to the water absorption band at 970 nm in Fig. 3.

This weakly absorbing model suggests that a high transmission of light through the louse might be expected. Measurement of light transmission does not show this. A typical transmission measurement indicates a maximum straight through transmission of only 6% (Fig. 4). The transmission curve has similar features to the reflection scan up to 850 nm but then continues with increasing transmission into the near infrared. This low straight through transmission indicates that the lice have strong light scattering properties. Strong scattering by a weakly absorbing sample will result in most of the light that enters the sample exiting it but diffusely rather than in any particular direction.

3.2. Scans of fish skin and attached sea lice

Sample spectral scans taken from skin and lice are shown in Fig. 5. These curves show two distinct groupings. The more reflective scans (the upper group of lines) are from the lighter regions of the fish close to and below the lateral line, and of the lice attached to these regions. The lower reflection scans are from the darker regions of the fish and lice on these areas. These data sets resemble those of the detached sea lice placed on the reflective surface and the carbon black paper respectively (Fig. 3). Visual comparison of the spectral shapes of the scans on the two regions is difficult due to the large differences in intensity. However, comparison is easier if these scans are normalised by dividing each scan by its average value. Significant differences between the scans of the lice on the light and dark regions are still apparent. Those on the light skin show more significant absorption bands, probably due to multiple scattering in the louse.

The upper group of curves in Fig. 5 clearly show a difference between the spectral response of the lice and the skin. This is particularly pronounced in the 700–850 nm region where the reflectance of the lice increases much more rapidly than the reflectance of the skin. There is much less difference between the scans of lice and fish skin taken in regions where the surface of the fish is dark.

3.3. Analysis of spectra to identify characteristic differences between lice and skin

A multivariate analysis technique known as Canonical Variate Analysis (Genstat 5 Committee, 1987) was used to quantify the differences between lice and fish skin spectral responses. The scans were first divided into those taken on the light areas

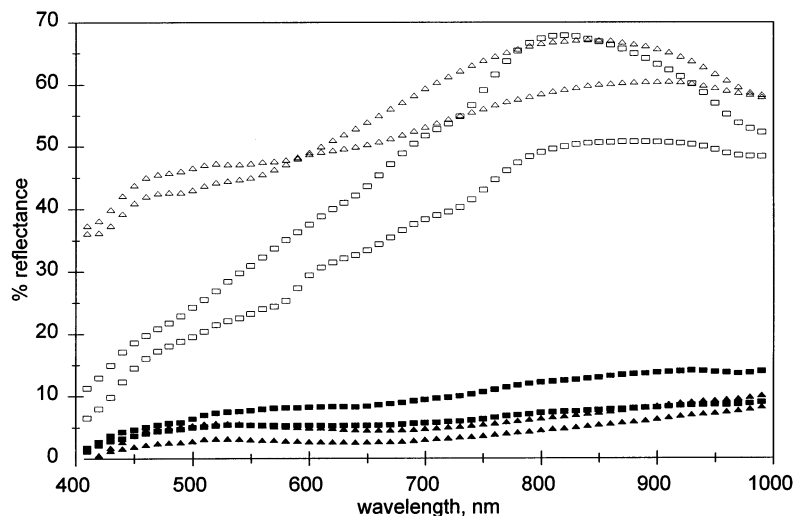


Fig. 5. Reflection scans of light (Δ) and dark (\blacktriangle) fish skin regions and of lice attached to light (\square) and dark (\blacksquare) areas of the fish.

(13 pairs of measurements) and those taken on the darker areas of the fish (17 pairs of measurements). This was done to maximise the chance of identifying spectral features that would enable discrimination in each of the broad categories.

The spectra were then smoothed to remove random noise. Most of the rapid changes in reflectance that can be seen in Fig. 3, for example, are due to noise signals and are unrelated to the optical properties of the sample object. These are particularly large at the low and high frequencies where the intensity of incident light was low. Measurement of the reflectance over a longer time would have reduced these substantially, however, new errors of a different nature might have been created as the sample was warmed by the light energy. Sampling errors can be reduced by smoothing the spectral scans. For this analysis, the spectra were smoothed over a 20 nm bandwidth, by replacing the reflectance at each wavelength R_λ with a local average R_λ^* which is calculated as:

$$R_\lambda^* = \frac{1}{11} \sum_{n=-5}^{n=5} R_{\lambda+2n} \quad (1)$$

where the wavelength of the light is λ and n enables a stepping through of the integrated wavelength band in the 2-nm intervals. The smoothed points were calculated at 10-nm intervals. To further reduce the influence of unreliable noisy data, the upper and lower wavelengths were truncated to limit the reflectance scans to wavelengths between 410 and 990 nm.

Four scans from each group of scans (lice on light areas, light skin, lice on dark areas, dark skin) were then randomly selected and reserved for testing the results of the analysis. The remaining scans were used to determine whether the spectral data could be separated into the predefined groups, salmon skin and lice. The canonical variate analysis (CVA) technique determines a linear combination of the reflectances at each wavelength that minimises the in-group variation (i.e. variation in the skin or lice scans) and maximises the between group variations. The canonical variate score S can then be calculated for each spectral scan. It is calculated as:

$$S = W_{\lambda_1} R_{\lambda_1} + W_{\lambda_2} R_{\lambda_2} + W_{\lambda_3} R_{\lambda_3} \dots W_{\lambda_n} R_{\lambda_n} \quad (2)$$

where R_{λ_1} is the reflection at the first wavelength of the range used in the CVA, R_{λ_n} is the reflectance at the last wavelength and W_{λ_n} is the weighting of that wavelength in the canonical variate vector.

Once these weightings have been calculated, they can be applied to the four sets of spectral scans from each group which were reserved for testing the analysis results. The canonical spectral scores for the training and test sets taken from the lighter skin areas are shown in Fig. 6. The training set is shown as squares, whereas the test set plotted as triangles. The training data clearly separate into the two predefined groups and the test set data are also well separated which confirms the validity of the separation. The weightings of the canonical variate are given in Fig. 7. This shows smooth and probably reliable features in the weightings between 600 and 900 nm that correspond to the differences in the spectral features observed in Fig. 5.

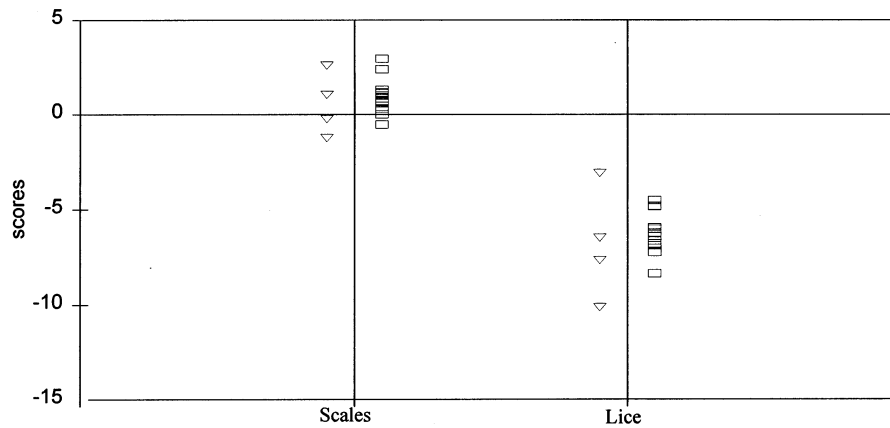


Fig. 6. Canonical variate scores for the training (□) and test set (▽) of smoothed spectral scans from the lighter regions for the lice/skin groupings.

The canonical scores for the training and test sets for the spectral scans taken from the darker areas of the fish are shown in Fig. 8. Although the separation here is poorer than on the light areas, separation has been achieved for the majority of scans. This is in agreement with the observations made on Fig. 5 where it was noted that the spectral differences between the lice scans and skin scans in these darker regions are smaller. The spectral weightings of the canonical vector in Fig. 9 show a smoothly varying feature only between 780 and 880 nm. This implies that much

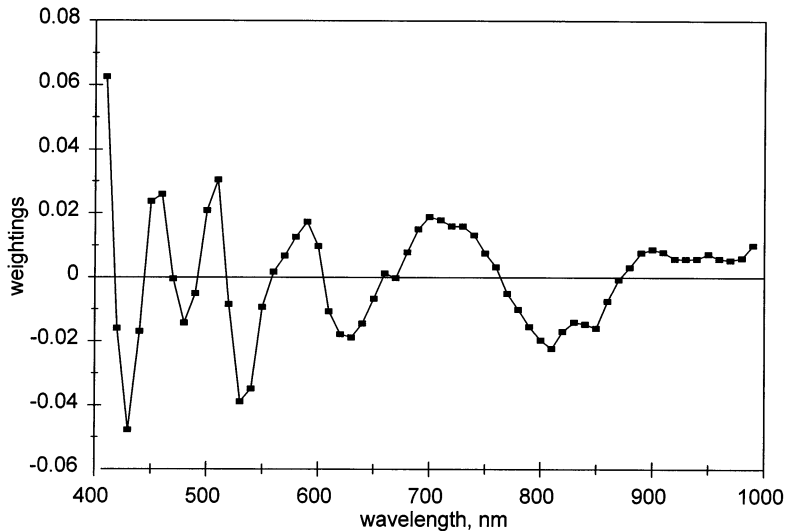


Fig. 7. The weightings W_{λ_n} of the canonical variate vector for the smoothed spectral scans obtained on the lighter regions of the fish.

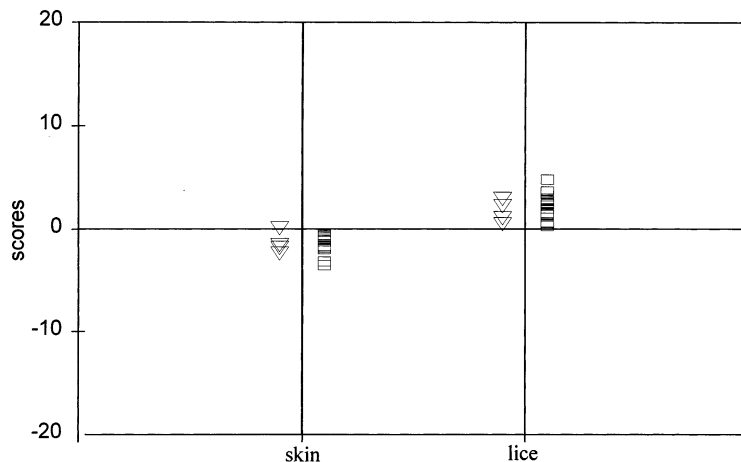


Fig. 8. Canonical variate scores for the training (\square) and test set (∇) of smoothed spectral scans from the darker regions for the lice/skin groupings.

of the separation between the lice and skin scans in the darker regions may be unreliable. One would expect from this that the separation of the test scans would be poorer than the training set. Fig. 8 gives some indication of this with one of the scores for the skin test set overlapping in value with the scores of the lice group.

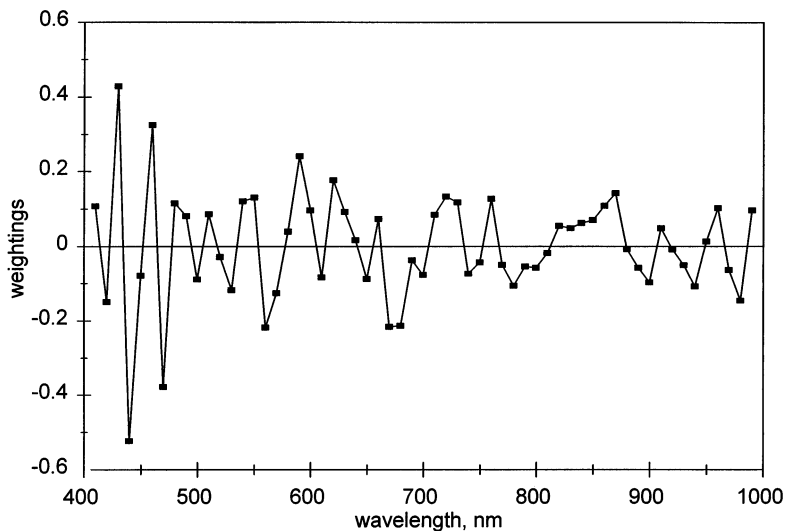


Fig. 9. The weightings W_{λ_n} of the canonical variate vector for the smoothed spectral scans obtained on the darker regions of the fish.

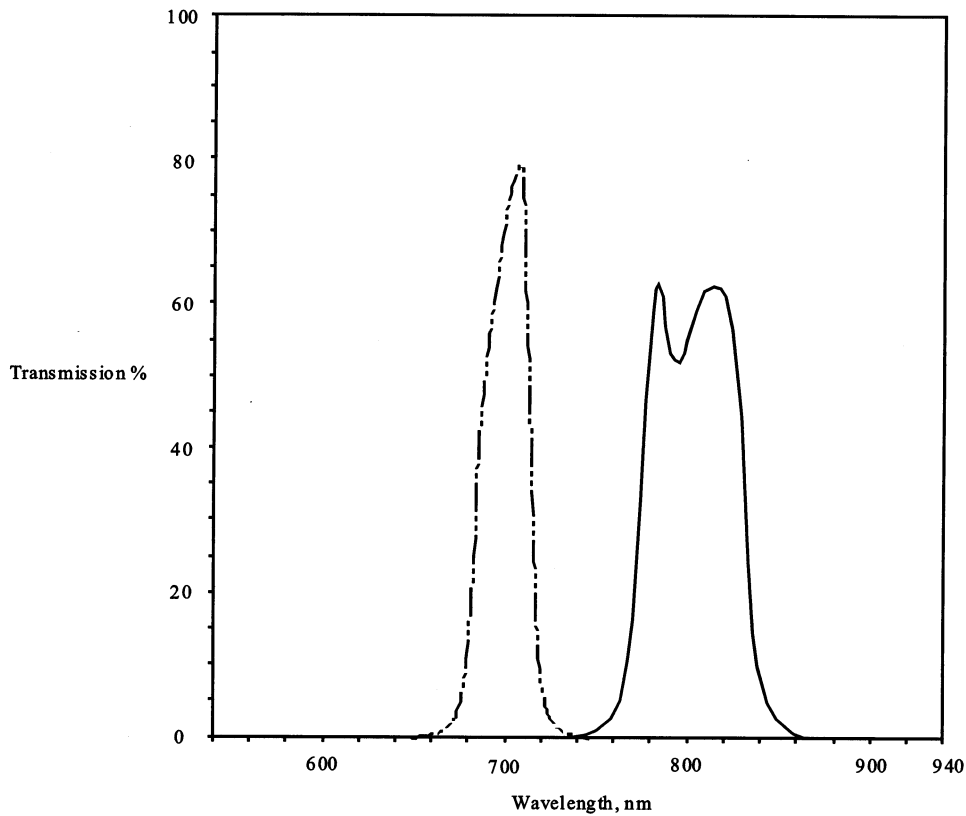


Fig. 10. Transmission characteristics of narrow band filters.

4. Collection of video images at selected wavelengths

Having identified differences in the spectra of the light reflected from the lice and salmon skin it was of interest to examine the potential for using video images to discriminate between salmon skin and lice on the basis of these differences. The clearest distinguishing feature between the spectra of the lice and skin on the lighter areas of the fish is the rise in reflectance between 700 and 800 nm, (Fig. 5). The weightings calculated in the Canonical Variate Analysis (see Fig. 7) show this feature as a strong downward slope from 700 to 800 nm. Video images of the salmon and lice were therefore collected at these wavelengths and processed to enhance this distinction.

The equipment used for collecting the images comprised a Pulnix monochrome camera with a 25 mm lens and a rotating filter holder connected to a Matrox Meteor frame grabber installed in a PC. The filters were narrowband glass filters from InfraRed Engineering with transmission characteristics as shown in Fig. 10. The camera was mounted approximately 80 cm above the fish surface, viewing the

fish in a controlled light chamber to ensure a reasonably constant and diffuse illumination level. Images of 768×576 pixels were collected with each filter, for a number of views of lice on the fish surface. One pair of images is shown in Fig. 11. The view is of the left side of the tail with the top surface of the fish on the right of the figure. Five lice are in the image, although not all are easily visible. These images were taken on the single salmon that was used to supply lice for the study of detached lice rather than that for which the Canonical Variate Analysis had been made.

5. Generation of synthesised image

The images taken at 700 and 800 nm were combined by taking the ratio of the grey levels of corresponding pixels as follows:

$$\begin{aligned} I_r [i,j] &= 128 \times \frac{I_7 [i,j]}{I_8 [i,j]} \quad \text{if } 0 < I_8 [i,j] \quad \text{and} \quad 128 \times \frac{I_7 [i,j]}{I_8 [i,j]} \leq 255 \\ &= 0 \quad \text{if } I_8 [i,j] = 0 \\ &= 255 \quad \text{if } 128 \times \frac{I_7 [i,j]}{I_8 [i,j]} > 255 \end{aligned} \quad (3)$$

where $I_7[i,j]$ is the grey level of the pixel in the i th column and j th row of the 700 nm image, $I_8[i,j]$ is the equivalent pixel in the 800 nm image and $I_r[i,j]$ is the equivalent pixel in the newly created ratio image. The scaling of the ratio assigns the grey level of 128 to a ratio of 1, with a ratio of 2 or above appearing as white (grey level 255). This creates a synthesised image which indicates by its grey levels the change in reflectance between wavelengths of 700 and 800 nm.

The synthesised image created from Fig. 11a and b is shown in Fig. 11c. A steep gradient in the spectrum should give a darker area in the ratio image. Three lice are quite clearly visible in the ratio image. There are two other lice present on the fish, marked in 11c by arrows, which are not so clearly shown. It is also of interest to notice how much the grey level variation of the rest of the fish surface has been reduced by the ratio technique.

The image in Fig. 11 shows the situation for lice close to the midline and on the tail fin. Lice on the underside of the fish showed greater contrast with the fish surface in all three images (700, 800 nm and the ratio image). Lice on the darker (dorsal) surface of the fish were difficult to see in any of the three images. These results are consistent with the results of the spectrum analysis described earlier. Fig. 9 shows little difference in weightings between 700 and 800 nm. Discrimination between lice and skin on this surface would probably be improved by using images taken at wavelengths of 780 and 870 nm.

Images were also collected of lice on the salmon with the fish immersed in a shallow tank of water, so that the water surface was just above the fish surface. This gave a flat air-to-water interface through which the fish was viewed, rather than the uneven surface given by a thin film of water over the fish. These images are likely

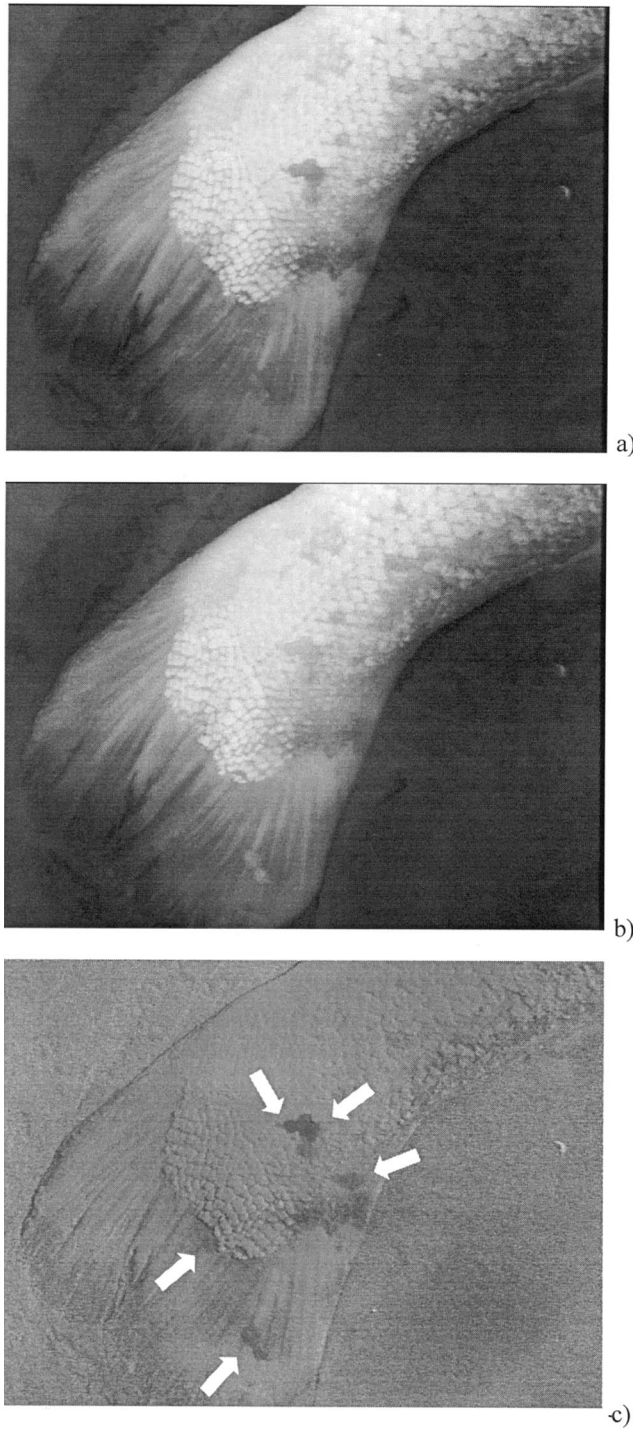


Fig. 11. Images of lice on a salmon (a) 700-nm image (b) 800-nm image (c) synthesised ratio image.

to be similar to those that would be collected by an underwater camera. The results of the images taken through the shallow water are similar to the results out of water, described above.

6. Future developments

Further work is required to improve discrimination of lice on the dark surfaces. Fig. 9 indicates that the most stable differences are to be found between 780 and 870 nm. Video images at these wavelengths need to be captured to demonstrate how well lice on the darker surfaces can be distinguished. Fig. 7 indicates that these wavelengths could also be suitable for discriminating lice on the lighter underside of fish.

One of the problems associated with moving to longer wavelengths is the increasing absorption of light by the water. Jerlov (1976) reports the transmittance of light through sea water to be 61% per metre at 700 nm, but only 9% at 750 nm and 18% at 800 nm. If the images are to be captured near the water surface, sensitive cameras may be needed to generate an adequate image. At any significant distance beneath the water surface additional light at the required frequencies may also be needed since this component of the sun light will not penetrate far into the water column. Rainbow trout and therefore probably Atlantic salmon are relatively insensitive to light at these wavelengths so such illumination need not be visible to the fish (Douglas, 1983).

The studies of the spectral properties of the detached lice indicated that the lice scattered light strongly. By using a directional light to illuminate the fish it is anticipated that the light reflected from the scales will be directional whereas the lice will appear as secondary and diffuse light sources on the surface of the fish. The potential of this technique for lice detection will be investigated further.

Automatic interpretation of the images has not yet been studied. However, techniques for identifying fish and tracing their outline have been developed (McFarlane and Tillet, 1997). A simple threshold technique could then be used to pick out the dark blobs of the lice, but this would also select some of the texture at scale edges, on the fins and at the edge of the fish. A more sophisticated detection algorithm would therefore probably be necessary. These images show, however, that there is potential to use a non-contact technique to help detect the presence of lice on the sides or under surface of salmon.

7. Conclusions

Examination of the spectral reflectance of sea lice and salmon skin has revealed distinguishing features in the reflectance spectrum which can be used to enhance the visibility of sea lice. These differences are particularly significant when the lice are attached to the lighter areas of the fish. This difference can be exploited using video images taken with band pass filters at light wavelengths of 700 and 800 nm. These

images can be combined to create a synthesised image with enhanced contrast between lice and salmon skin and reduced contrast due to other variations in surface colour. Discrimination of the lice on dark surfaces is more difficult but may be enhanced using longer wavelengths of light (780 and 870 nm). Sea lice are found to scatter light strongly. This might also be used to enhance the visibility of lice on the darker areas of skin.

Further work is required to assess the potential of this technique for underwater inspection of free swimming salmon. Automatic interpretation of the images which would supply an estimate of the lice burden may be possible but it has not yet been investigated.

Acknowledgements

This work was supported by the Biotechnology and Biological Sciences Research Council of Great Britain. The authors gratefully acknowledge the assistance of Marine Harvest McConnell in this investigation and in particular that of David Mitchell, Simon Wadsworth and John Muckhart.

References

- Bakke Jøssund, T.J., 1995. Lusetelling som led i helsetjeneste for fiskeoppdrett. *Norske Veterinærtidsskrift* 107 (2), 114–119.
- Bull, C.R., Mottram, T., Wheeler, H.C., 1995. Optical teat inspection for automatic milking systems. *Computers and Electronics in Agriculture* 12, 121–130.
- Bull, C.R., 1990. A model of the reflectance of near infra-red radiation. *Journal of Modern Optics* 37, 1955–1964.
- Bull, C.R., 1991. Compensation for particle size effects in near-infrared reflectance. *The Analyst* 116, 781–786.
- Bull, C.R., 1993. A Review of sensing techniques which could be used to generate images of agricultural and food materials. *Computers and Electronics in Agriculture* 8, 1–29.
- Douglas, R.H., 1983. Spectral sensitivity of rainbow trout (*Salmo gairdneri*). *Rev. Can. Biol. Exp.* 42 (2), 117–122.
- Genstat 5 Committee, 1987. *Genstat 5 Reference Manual*. Oxford Science Publications, pp. 449–531.
- Grimnes, A., Jakobsen, P.J., 1996. The physiological effects of salmon lice infection on post-smolt of Atlantic salmon. *Journal of Fish Biology* 48 (6), 1179–1194.
- Hecht, E., Zajac, A., 1979. *Optics*, 4th edn. Addison Wesley, Reading.
- Jackson, D., 1998. Developments in sea lice management in Irish salmon farming. *Caligus*, 4, December 1998, a newsletter funded under the EU Fair programme.
- Jerlov, N.G., 1976. *Marine Optics*. Elsevier, Amsterdam, p. 52.
- Johnson, S.C., Albright, L.J., 1991. The developmental stages of *Lepeophtheirus salmonis*. *Canadian Journal of Zoology* 69 (4), 929–950.
- Kvenseth, P.G., 1997. Best current practice for lice control in Norway. *Caligus*, 2, December, 1997, a newsletter funded under the EU FAIR program.
- McFarlane, N.J.B., Tillett, R.D., 1997. Fitting 3D point distribution models of fish to stereo images. In: *BMVC97 Proceedings of the 8th British Machine Vision Conference*, 8–11 September 1997. University of Essex, UK, vol. 1, pp. 330–339.

- Mohesenin, N.N., 1984. *Electromagnetic Radiation Properties of Food Agricultural Products*. Gordon and Breach, London.
- Schram, T.A., 1993. Livssyklus hos lakselus, *Lepeophtheirus salmonis*; stadienes utseende og biologi. *Norsk Veterinaertidsskrift* 105 (12), 1207–1215.
- Sinnott, R. 1998. Sea lice, watch the hidden costs. *Fish Farmer*, October.
- Smith, P.D., 1999. *Fish and Shellfish Cultivation and Health Review: Report of the Assessor for Fish and Shellfish Health*. MAFF, London.
- Treasurer, J.W., Grant, A., 1998. The Marine Harvest McConnell surveillance system for sea lice infesting farmed Atlantic salmon, *Caligus* 4 December 1998, a newsletter funded under the EU Fair programme.